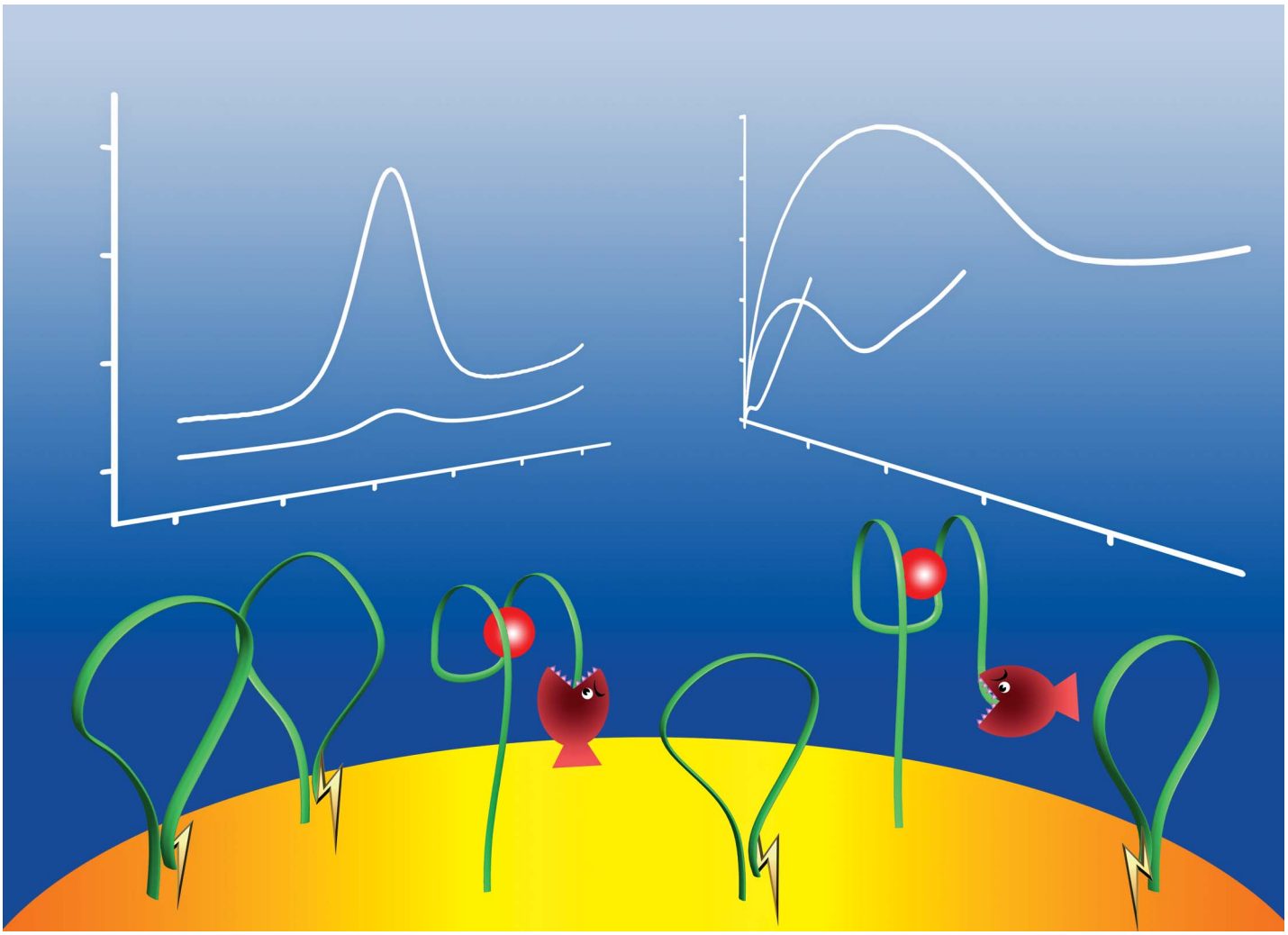

Showcasing research on exonuclease-assisted electrochemical determination of potassium levels from Peng Miao at CAS Key Lab of Bio-Medical Diagnostics, Suzhou Institute of Biomedical Engineering and Technology, Chinese Academy of Sciences, Suzhou, China.

Title: An aptasensor for detection of potassium ions based on $RecJ_f$ exonuclease mediated signal amplification

An electrochemical biosensor for the detection of potassium ions has been developed using a designed DNA probe. An aptamer sequence within the DNA probe is employed as the recognition element and the stem–loop structure is designed for the K^+-assisted conformational switch and the following RecJf exonuclease cleavage.

As featured in:

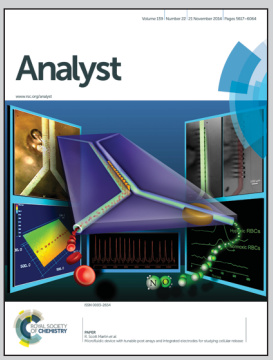

See Peng Miao *et al.*, *Analyst*, 2014, **139**, 5695.

ROYAL SOCIETY OF CHEMISTRY

www.rsc.org/analyst

Registered charity number: 207890

Analyst

PAPER

View Article Online
View Journal | View Issue

Cite this: *Analyst*, 2014, **139**, 5695

An aptasensor for detection of potassium ions based on $RecJ_f$ exonuclease mediated signal amplification

Peng Miao,*[ab] Yuguo Tang,[ab] Bidou Wang,[a] Kun Han,[ab] Xifeng Chen[a] and Haixuan Sun[ab]

Received 23rd July 2014
Accepted 16th September 2014

DOI: 10.1039/c4an01350f

www.rsc.org/analyst

An electrochemical biosensor for potassium has been developed combining specific potassium–aptamer binding and $RecJ_f$ exonuclease mediated signal amplification. Generally, the DNA probe with a stem-loop structure containing an anti-K^+ aptamer sequence is designed and modified on a gold electrode. K^+ can specifically bind to the aptamer and a G-quadruplex structure forms, which breaks the original stem-loop structure. The induced single-stranded 5′ end can be further digested by $RecJ_f$ exonuclease, releasing K^+ which can bind to another DNA probe on the electrode. After cycles of $RecJ_f$ exonuclease cleavage initiated by K^+, the electrochemical signal intensity is significantly decreased, and can be used to determine the concentration of K^+. This aptasensor shows high sensitivity, selectivity as well as excellent stability and accuracy, which provides possibilities for further applications of K^+ assay in clinical diagnosis.

Introduction

Potassium is one of the essential elements in living organisms, which plays important roles in the cardiovascular system, nerve transmission, muscular strength maintenance and so on.[1,2] Abnormal K^+ levels can be observed as a symptom of many diseases including diabetes, cancer, alcoholism and cardiovascular diseases.[3–5] Therefore, accurately monitoring the potassium level is crucial for clinical analysis.

Recently, a diversity of analytical methods, such as atomic absorption spectroscopy (AAS), inductively coupled plasma-mass spectrometry (ICP-MS), capillary electrophoresis, and fluoroionophore based sensing,[6–8] have been reported for the detection of K^+. Nevertheless, there are still problems to be solved. Most of the above mentioned methods require sophisticated instrumentation, some are tedious with complicated laboratory procedures, and some may suffer disadvantages of low sensitivity and a narrow detection range. Thereby, developing simple and sensitive detection methods is still highly desired.

Aptamers are artificial single-stranded DNA or RNA molecules that are able to target various analytes with high affinity and specificity.[9,10] Generally, they are selected through systematic evolution of ligands by exponential enrichment (SELEX). Owing to the unique properties of oligonucleotides, aptamers exhibit several advantages over other ligands including antibodies. *In vitro* synthesis and modification of aptamers are easy and cost-effective. The binding affinities with different targets are usually much high and aptamers are thermally stable. Therefore, aptamers have been broadly used in the fabrication of biosensors for the detection of small molecules, proteins and even whole cells.[11–13] Moreover, they can also be used as therapeutic agents since they have little or no immunogenicity.[14]

In this work, we have developed an electrochemical aptasensor for detection of K^+ ions. Electrochemical methods have many merits such as high sensitivity, low cost, ease of signal quantification and so on,[15–17] which may overcome certain disadvantages of currently used K^+ assays mentioned above. The designed procedure of the aptasensor is depicted in Scheme 1. A DNA probe with a stem-loop structure containing an anti-K^+ aptamer sequence is synthesized. The 3′ end thiol group of the DNA probe helps the immobilization on the gold electrode surface[18,19] and the 5′ end methylene blue (MB) provides significant electrochemical signals.[20] K^+ is capable of promoting the transformation of the guanine (G)-rich single-stranded aptamer to the G-quadruplex *via* intramolecular hydrogen bonding.[21] Thus, the stem part of the DNA is broken, releasing the single-stranded 5′ end. Since $RecJ_f$ is a single-stranded DNA specific exonuclease, the DNA can be digested with the K^+-assisted conformational switch. During the cleavage process, K^+ is released back to the solution and can be recognized by another DNA probe on the electrode, which initiates a new cycle of $RecJ_f$ exonuclease cleavage. Due to the departure of a large number of MB molecules, significant decrease of the electrochemical signals can be observed. By taking advantage of

[a]*CAS Key Lab of Bio-Medical Diagnostics, Suzhou Institute of Biomedical Engineering and Technology, Chinese Academy of Sciences, Suzhou 215163, P. R. China. E-mail: miaopeng@sibet.ac.cn; Fax: +86 512 69588283; Tel: +86 512 69588279*

[b]*University of Chinese Academy of Sciences, Beijing 100049, P. R. China*

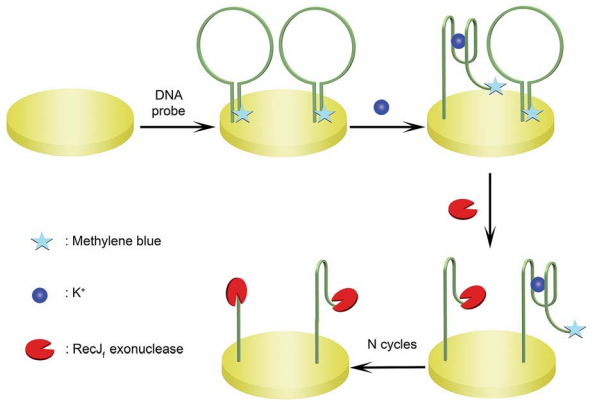

Scheme 1 Illustration of the aptasensor for K^+ with $RecJ_f$ exonuclease mediated signal amplification.

specific potassium–aptamer binding and $RecJ_f$ exonuclease mediated signal amplification, sensitive and selective detection of K^+ can be achieved.

Experimental

Reagents and chemicals

$RecJ_f$ exonuclease was obtained from New England Biolabs Ltd (Beijing, China). Hexaammineruthenium(III) chloride ($[Ru(NH_3)_6]^{3+}$), tris(2-carboxyethyl)phosphine hydrochloride (TCEP) and mercaptohexanol (MCH) were purchased from Sigma-Aldrich (USA). A 100 bp DNA ladder was supplied by TIANGEN Biotech Co., Ltd (Beijing, China). Other reagents were of analytical reagent grade and used as received. Human urine and serum samples were from healthy individuals. DNA oligonucleotides modified with thiol groups and MB were synthesized and purified by Sangon Biotech Co., Ltd (Shanghai, China). The sequence was 5′-MB-AAA*GGTTGGTGTGGTTGG*AACCTTT-$(CH_2)_3$-SH-3′. The italic part is the aptamer sequence specific for potassium ions[22] and the underlined parts are complementary sequences which could help in the formation of the stem-loop structure. All the solutions were prepared with ultrapure water that was purified with a Milli-Q purification system (Branstead, USA).

Preparation of the DNA modified electrode

Prior to the modification, the substrate gold electrode was firstly incubated in piranha solution (98% H_2SO_4–30% H_2O_2 = 3 : 1) for 5 min to eliminate any adsorbed materials (**Caution**: piranha solution reacts violently with organic matter). The electrode was then abraded with sand paper and polished with alumina powder (Al_2O_3) of different sizes (1.0, 0.3, and 0.05 μm) to mirror smoothness. Afterward, it was sonicated for 5 min in ethanol and water, respectively. The electrode was further soaked in 50% nitric acid for 30 min and then electrochemically cleaned in 0.5 M H_2SO_4 with scanning between 0 and 1.6 V for 20 cycles. The DNA probe was heated to 90 °C for 5 min and cooled slowly to room temperature. The immobilization of the DNA with the stem-loop structure on the gold electrode was achieved by incubating the electrode in 2 μM DNA for 8 h. Subsequently, the electrode was treated with 1 mM MCH for 30 min to obtain a well-aligned DNA monolayer.[23]

K^+-assisted exonuclease cleavage

The DNA modified electrode was immersed in the mixture of K^+ and $RecJ_f$ exonuclease solution (1 unit μL^{-1}, 50 mM NaCl, 10 mM Tris–HCl, 10 mM $MgCl_2$, 1 mM DTT, pH 7.9) at 37 °C for 1 h. The concentration of K^+ was from 50 nM to 1 mM. Afterward, the reaction was terminated by heating to 65 °C for 20 min.

Electrochemical measurements

All electrochemical experiments were conducted using a CHI660D workstation (CH Instruments, Shanghai, China) at room temperature (25 ± 2 °C). A conventional three-electrode system was employed, which consisted of a platinum auxiliary electrode, a saturated calomel reference electrode (SCE) and a DNA modified gold electrode as the working electrode (Φ = 3 mm). Chronocoulometry (CC) was carried out in 10 mM Tris–HCl with 50 μM $[Ru(NH_3)_6]^{3+}$ (pH 7.4). Electrochemical impedance spectra (EIS) measurements were performed in 5 mM $Fe(CN)_6^{3-/4-}$ with 1 M KNO_3. Square wave voltammetry (SWV) was conducted in 20 mM Tris–HCl (pH 7.5). Experimental parameters were as follows: for CC, pulse period (250 ms); for EIS, bias potential (0.204 V *versus* SCE), amplitude (5 mV), and frequency range (1–100 000 Hz); for SWV, amplitude (25 mV), step potential (4 mV), and frequency (50 Hz).

Gel electrophoresis assay

DNA samples before and after $RecJ_f$ exonuclease cleavage were also monitored for comparison by 4% agarose gel electrophoresis for 30 min (120 V). The gel stained with ethidium bromide was photographed under UV light by using a Gel Doc™ XR+ System (Bio-Rad, USA).

Results and discussion

Quantitation of DNA density on the electrode surface

Chronocoulometry is employed to provide the information of DNA density on the electrode by detecting the electrochemical signal of $[Ru(NH_3)_6]^{3+}$.[24] As shown in Fig. 1, the chronocoulometry curves before and after the DNA modification are recorded. The accurate amount of $[Ru(NH_3)_6]^{3+}$ can be obtained by referring to the Cottrell equation as indicated in our previous work,[25] and the surface density of DNA is calculated to be 9.3 ± 0.4 pmol cm^{-2}.

Electrochemical characterization

The whole process of the proposed aptasensor including the assembly of DNA on the electrode, the formation of a rigid G-quadruplex with K^+ and $RecJ_f$ exonuclease cleavage can be characterized by EIS (Fig. 2). As is well known, a larger semicircle diameter in an impedance spectrum usually indicates a larger interfacial charge transfer resistance. It can be observed that the bare gold electrode includes no semicircle domain (curve A). After DNA modification, due to the negatively charged

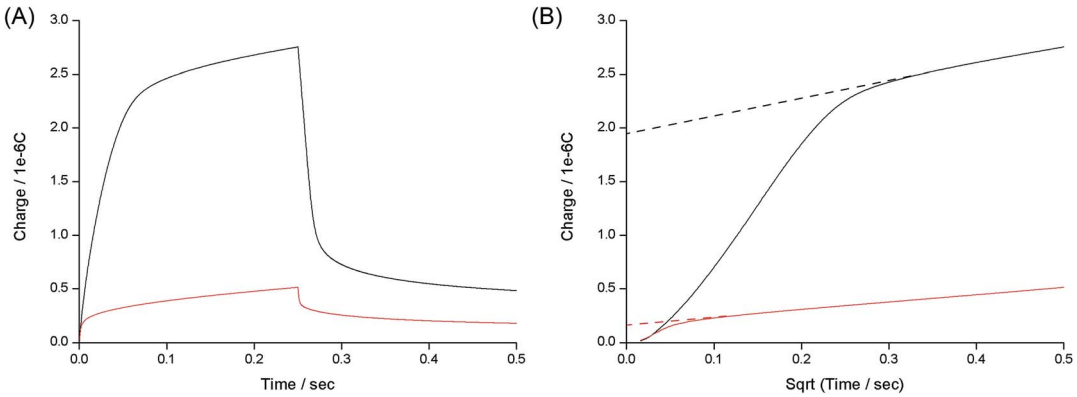

Fig. 1 (A) Chronocoulometry curves for the gold electrodes modified with MCH (bottom) and DNA before MCH (top). (B) Shows the chronocoulometry curves of charge *versus* $t^{1/2}$.

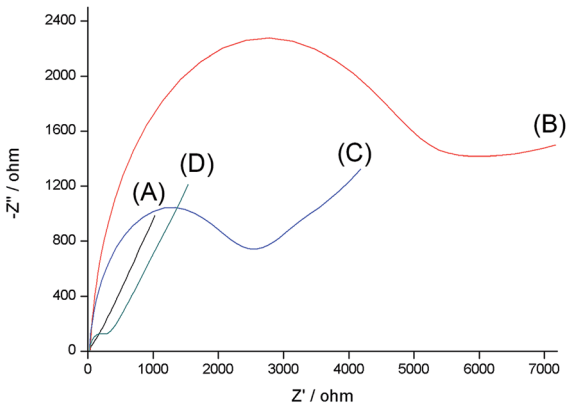

Fig. 2 Nyquist plots corresponding to (A) bare gold electrode, (B) DNA modified electrode, (C) DNA modified electrode after incubation in 1 mM KCl for 1 h, and (D) DNA modified electrode after $RecJ_f$ exonuclease cleavage in the presence of 1 mM KCl.

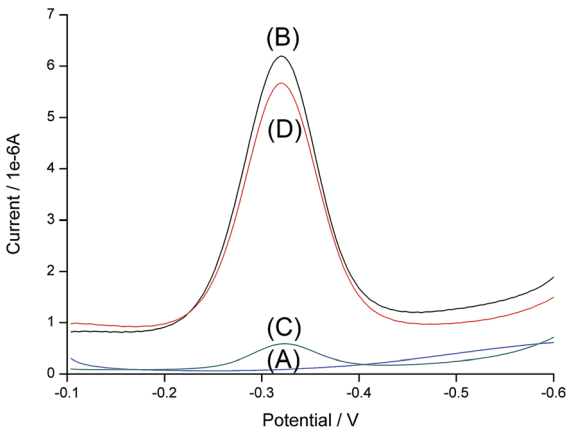

Fig. 3 Square wave voltammograms corresponding to (A) bare electrode, (B) DNA modified electrode, and (C and D) after exonuclease cleavage in the presence and absence of 1 mM K^+.

phosphate backbone that can electrostatically repel $Fe(CN)_6^{3-/4-}$, interfacial charge transfer is inhibited and the semicircle increases significantly (curve B). As the positively charged K^+ can be encapsulated in the rigid G-quadruplex, the semicircle decreases (curve C). After the $RecJ_f$ exonuclease cleavage, the DNA probes on the electrode are largely shortened and the repellency effect declines sharply (curve D). The EIS results have confirmed well the aptasensor mechanism.

In addition, the electrochemical properties of the modified electrode are studied by SWV. As shown in Fig. 3, the bare electrode displays no current peak. After DNA modification, the attached MB molecules attribute to a peak at −0.32 V. In the absence of K^+, $RecJ_f$ exonuclease cannot effectively digest the DNA probe on the electrode, and the peak is nearly unchanged.

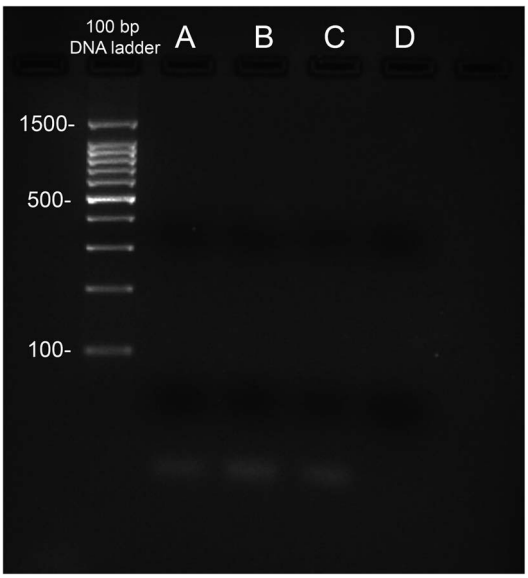

Fig. 4 Agarose gel electrophoresis analysis: (A) DNA; (B) DNA digested by $RecJ_f$ exonuclease without K^+; (C) DNA and K^+; (D) DNA digested by $RecJ_f$ exonuclease in the presence of K^+ (DNA: 75 ng; $RecJ_f$ exonuclease: 15 unit; K^+: 10^{-6} μmol).

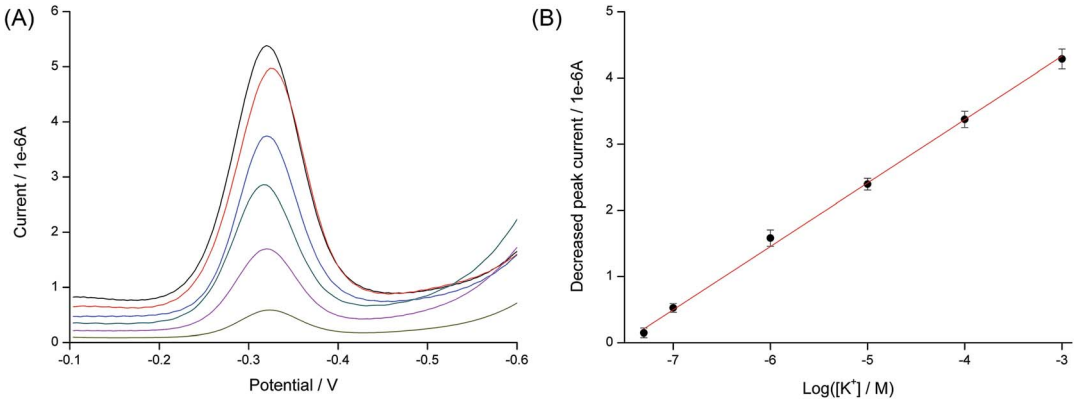

Fig. 5 (A) Square wave voltammograms corresponding to the DNA modified electrode after $RecJ_f$ exonuclease cleavage in the presence of 50 nM, 100 nM, 1 μM, 10 μM, 100 μM, and 1 mM K^+ (from top to bottom). (B) Calibration curve of decreased peak current *vs.* logarithmic K^+ concentration. The error bars represent standard deviations of three independent measurements.

However, K^+ helps the release of the single-stranded 5′ end which is specific for $RecJ_f$ exonuclease and a significant decrease of peak current is then induced.

Gel electrophoresis characterization

The oligonucleotide cleavage behaviour by $RecJ_f$ exonuclease during the assay is also studied by gel electrophoretic analysis. Since only one DNA probe is employed in the experiments, agarose gel electrophoretic assay is performed, which is sensitive enough to distinguish the cleavage behaviour. Lane A in Fig. 4 is the DNA band without exonuclease cleavage. Lane B and C show the bands of DNA mixed with K^+ and $RecJ_f$ exonuclease, respectively. However, after the incubation with both K^+ and $RecJ_f$ exonuclease, no DNA band can be observed (Lane D), which suggests that the exonuclease cleavage reaction of the stem-loop DNA occurs under a K^+-assisted conformation switch.

Sensitivity and selectivity

The concentration of K^+ is quantified by measuring the electrochemical signals of SWV experiments. As is expected, Fig. 5 shows that the increase in the concentration of K^+ results in the gradual reduction of the current peak. The decreased signal intensity is linearly related to the logarithmic concentration of K^+ in the range from 50 nM to 1 mM. The regression equation is $y = 7.21 + 0.96x$, in which y is the decreased peak current, x is the logarithmic concentration of K^+, and $R^2 = 0.99$. The detection limit of the measurements is calculated to be 50 nM (3σ). The average coefficient of variation is 4.83%.

To evaluate the selectivity of the proposed aptasensor strategy for K^+, Na^+, Ag^+, Ca^{2+}, Fe^{2+}, Fe^{3+}, Zn^{2+}, Al^{3+} have been employed as the potential interference ions, each at the concentration of 20 mM. Fig. 6 clearly shows that little change of the current peak is observed with different interference ions and a significant decrease can be observed only in the presence of K^+. These results confirm the excellent selectivity of this aptasensor for K^+.

Determination of K^+ in urine samples

The practicality of the proposed method in real samples is then checked. Since K^+ levels in serum or urine are indicative information for certain diseases and have clinical significances,[26] we detected the K^+ concentration in human urine and serum

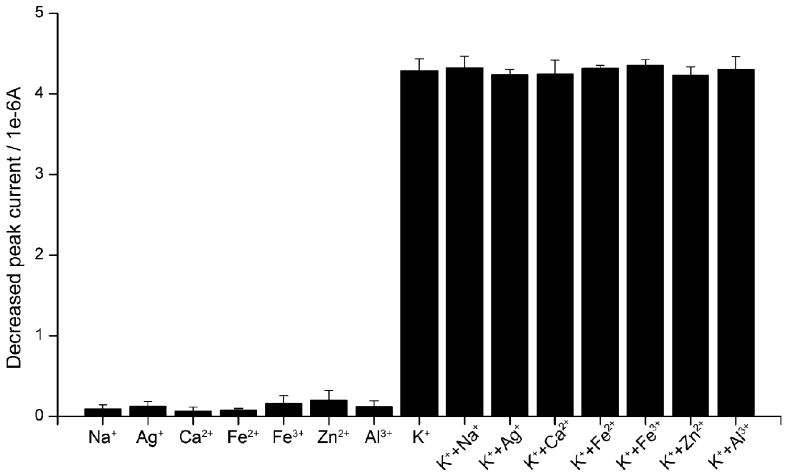

Fig. 6 Selectivity of the K^+ aptasensor against a range of other ions (20 mM). The concentration of K^+ is 1 mM.

Table 1 Analytical results for K^+ detection in urine and serum samples by the proposed aptasensor and AAS

Sample	Aptasensor (mM)	AAS (mM)	Added (mM)	Found (mM)	Recovery (%)
Urine 1	30.5	29.7	10	11.2	112
Urine 2	54.1	55.2	10	9.5	95
Urine 3	73.2	73.8	10	9.7	97
Serum 1	3.9	4.1	10	9.8	98
Serum 2	4.6	4.4	10	10.4	104
Serum 3	5.1	5.2	10	9.6	96

samples under the same detection procedure as described in the aforementioned experiments. The samples were previously filtered and diluted 100-fold before the measurements. As listed in Table 1, the detection results by the proposed aptasensor are compared with AAS results and show fairly good concordance. Satisfactory recoveries are also achieved. The effectiveness of the proposed method in real samples is thus well confirmed.

Conclusions

In conclusion, a simple, sensitive and selective electrochemical aptasensor for K^+ is developed. The aptamer sequence within the DNA probe is used as the recognition element and the stem-loop structure is designed for the K^+-assisted conformational switch and the following $RecJ_f$ exonuclease cleavage. A detection limit as low as 50 nM is achieved. In addition, this aptasensor shows little interference from other ions and good feasibility in application in real samples, which is promising for broad potential use in clinical applications.

Acknowledgements

This work was supported by the National Key Instrument Developing Project of China (Grant no. ZDYZ2013-1) and the Natural Science Foundation of Jiangsu Province of China (Grant no. BK20141204).

References

1 F. J. He and G. A. MacGregor, *Physiol. Plant.*, 2008, **133**, 725–735.
2 S. Sawai, S. Misawa, K. Kanai, S. Isose, K. Shibuya, Y. Noto, Y. Fujimaki, Y. Sekiguchi, S. Nasu, F. Nomura and S. Kuwabara, *Clin. Neurophysiol.*, 2011, **122**, 205–209.
3 C. S. Chan and D. J. Surmeier, *Nat. Neurosci.*, 2014, **17**, 641–642.
4 M. L. Garcia and G. J. Kaczorowski, *Curr. Opin. Pharmacol.*, 2014, **15**, 1–6.
5 Q. Zhang, R. Ramracheya, C. Lahmann, A. Tarasov, M. Bengtsson, O. Braha, M. Braun, M. Brereton, S. Collins, J. Galvanovskis, A. Gonzalez, L. N. Groschner, N. J. G. Rorsman, A. Salehi, M. E. Travers, J. N. Walker, A. L. Gloyn, F. Gribble, P. R. V. Johnson, F. Reimann, F. M. Ashcroft and P. Rorsman, *Cell Metab.*, 2013, **18**, 871–882.
6 F. G. Lepri, E. S. Chaves, M. A. Vieira, A. S. Ribeiro, A. J. Curtius, L. C. C. De Oliveira and R. C. De Campos, *Appl. Spectrosc. Rev.*, 2011, **46**, 175–206.
7 H. R. He, M. A. Mortellaro, M. J. P. Leiner, R. J. Fraatz and J. K. Tusa, *J. Am. Chem. Soc.*, 2003, **125**, 1468–1469.
8 J. Tanyanyiwa and P. C. Hauser, *Anal. Chem.*, 2002, **74**, 6378–6382.
9 C. C. Huang, Y. F. Huang, Z. H. Cao, W. H. Tan and H. T. Chang, *Anal. Chem.*, 2005, **77**, 5735–5741.
10 I. Willner and M. Zayats, *Angew. Chem., Int. Ed.*, 2007, **46**, 6408–6418.
11 M. C. Rodriguez, A. N. Kawde and J. Wang, *Chem. Commun.*, 2005, 4267–4269.
12 Y. Shi, H. C. Dai, Y. J. Sun, J. T. Hu, P. J. Ni and Z. Li, *Analyst*, 2013, **138**, 7152–7156.
13 L. M. Qu, J. H. Xu, X. F. Tan, Z. Liu, L. G. Xu and R. Peng, *ACS Appl. Mater. Interfaces*, 2014, **6**, 7309–7315.
14 O. C. Farokhzad, J. J. Cheng, B. A. Teply, I. Sherifi, S. Jon, P. W. Kantoff, J. P. Richie and R. Langer, *Proc. Natl. Acad. Sci. U. S. A.*, 2006, **103**, 6315–6320.
15 C. K. Gu, H. Xu, M. Park and C. Shannon, *Langmuir*, 2009, **25**, 410–414.
16 P. Miao, *RSC Adv.*, 2013, **3**, 9606–9617.
17 Y. Cao, S. Zhu, J. C. Yu, X. J. Zhu, Y. M. Yin and G. X. Li, *Anal. Chem.*, 2012, **84**, 4314–4320.
18 P. Miao, L. M. Ning, X. X. Li, P. F. Li and G. X. Li, *Bioconjugate Chem.*, 2012, **23**, 141–145.
19 Y. Cao, J. C. Yu, B. Bo, Y. Q. Shu and G. X. Li, *Biosens. Bioelectron.*, 2013, **45**, 1–5.
20 R. Freeman, Y. Li, R. Tel-Vered, E. Sharon, J. Elbaz and I. Willner, *Analyst*, 2009, **134**, 653–656.
21 B. Kim, I. H. Jung, M. Kang, H. K. Shim and H. Y. Woo, *J. Am. Chem. Soc.*, 2012, **134**, 3133–3138.
22 X. L. Zhu, J. Zhao, Y. Wu, Z. M. Shen and G. X. Li, *Anal. Chem.*, 2011, **83**, 4085–4089.
23 P. Miao, L. Liu, Y. Li and G. X. Li, *Electrochem. Commun.*, 2009, **11**, 1904–1907.
24 A. B. Steel, T. M. Herne and M. J. Tarlov, *Anal. Chem.*, 1998, **70**, 4670–4677.
25 P. Miao, L. M. Ning and X. X. Li, *Anal. Chem.*, 2013, **85**, 7966–7970.
26 I. Grgic, E. Kiss, B. P. Kaistha, C. Busch, M. Kloss, J. Sautter, A. Muller, A. Kaistha, C. Schmidt, G. Raman, H. Wulff, F. Strutz, H. J. Grone, R. Kohler and J. Hoyer, *Proc. Natl. Acad. Sci. U. S. A.*, 2009, **106**, 14518–14523.